

A FURTHER STUDY OF RELATIVE LONGITUDE SHIFT OF PULSAR BEAMS

R. X. XU, J. W. XU, G. J. QIAO

CAS-PKU JOINT BEIJING ASTROPHYSICAL CENTER AND DEPARTMENT OF ASTRONOMY,
 PEKING UNIVERSITY, BEIJING 100871, CHINA

Draft version December 2, 2024

ABSTRACT

It is of great important to study pulsar beam shapes if we are concerned with emission theories and pulsar birth rate. Both observations^[9, 16] and/or the ICS model^[10] show that different emission components are emitted from different heights. The relative longitude phase shifts due to different heights of emission components and to the toroidal velocity of electron are considered in this paper. Several possible observational features arising from the phase shift effects are presented. The emission beams may not have circular cross sections although the emission regions may be symmetric with respect to the magnetic axes.

Subject headings: pulsars — polarization — radiation mechanisms

1. INTRODUCTION

Soon after the discovery of Pulsars, the rotating vector model (RVM) was proposed to well explain the linear polarization characteristics of pulsar radio emission, in which Radhakrishnan and Cooke^[1] assumed that relativistic particles stream out along dipolar magnetic fields of pulsars and the polarization position angle of emitted radiation from these particles is correlated with the magnetic curvature. Theoretical extensions of the RVM have appeared in literatures (e.g., Ferguson^[2], Blaskiewicz et. al.^[3], Hirschman & Arons^[4]), where some detailed physical factors, such as the special relativistic effects, the polar-cap current flow, have been included.

However the RVM fails in attempting to explain the position angle jumps observed in mean pulses as well as in individual pulses^[5]. This leads to the assumption that the radio beams of pulsars contain two nearly orthogonal polarization modes, the superposition of which results in the non-S-shaped position angle variation in mean pulses and two $\sim 90^\circ$ separated distributions of position angles in individual pulses (see the paper by Mckinnon & Stinebring^[6] and references therein). Nevertheless, there is still a possibility that modified RVM, *without* inclusion of the orthogonal modes, can reproduce the observed position angle “jumps” if we consider the linear depolarization of pulsar beams and the observational uncertainties originated from observation polarimeters^[7, 8]. In view of the observational fact that radio emission of pulsars may have three components (core and two

cones) which are emitted from different heights above pulsar surface^[9], Xu et al.^[7] found that the position angles of mean pulses jump at certain longitudes where the linear polarization is approximately zero if the retardation effect, which causes the beam centers to be shifted between each other, can significantly conduce toward the linear depolarization. In this paper, we further study this issue arising from different emission heights which are calculated according to the inverse Compton scattering model^[10] in which core and conal components can be naturally reproduced.

Besides the polarization effect discussed above, different emission heights may also have notable consequence to beam shapes. Many authors investigated observationally the pulsar beam shapes, the previous results of which are summarized below. Jones^[11] find that the latitudinal radius of beam cross section could be 2.5 times the longitudinal one. Narayan & Vivekanand^[12] modify this ratio to be 3.0. Lyne & Manchester's^[13] conclusion is that the shape of the emission beam is approximately circular. Biggs^[14] proposes that there may be some meridional compression. Wu & Shen^[15] find that, for pulsars with short period, the radius of the emission beam at latitudinal direction is larger. However, the latitudinal radius is smaller for pulsars with longer period. Rankin, therefore, change her morphological beam shape from an elliptical cross section^[9] to a circular one^[16]. Our numerical results in section 3 may be checked by such observational study in the future. We find that the

¹email: rxxu@bac.pku.edu.cn, xjw@bac.pku.edu.cn, gjn@pku.edu.cn

²This work is supported by NSFC (No. 19803001), by the Special Funds for Major State Basic Research Project, and by Doctoral Program Foundation of Institution of Higher Education in China.

emission beams of pulsars with small rotation periods do not have circular cross sections even if the emission regions are symmetric with respect to the magnetic axes if we take into account the toroidal velocity due to rotation.

This paper is organized as below. After inspecting various aspects of the retardation effect caused by different emission heights and their possible observational consequences in section 2, we calculate the emission beams from relativistic particles with poloidal (along magnetic field lines) and toroidal (perpendicular to field lines) velocities in section 3. A conclusion, based on which we can know the phase shift between two emission units at arbitrary positions, is proved geometrically in Appendix. The paper is summarized in section 4.

2. RELATIVE LONGITUDE SHIFT DUE TO DIFFERENT HEIGHTS

It is generally believed that pulsars' radio emission is originated from the region near the last open field lines. We assume in this section that the particles in the last-open-field-line region, which are responsible to observed radiation, have only poloidal velocities along the field lines (i.e., the toroidal velocity is neglected), and are accelerated symmetrically respect to the magnetic axis. The emission region of each beam component is thus also symmetric respect to the axis. According to Appendix, the phase shifts of all emission elements of a certain beam component is the same since the values $\mathbf{r} \cdot \mathbf{n}_0$ of those emission elements are the same, where \mathbf{r} is the vector position of an element, \mathbf{n}_0 the emission direction. Therefore the emission beams should have circular cross sections in this case.

2.1. Emission heights and beam shift

We know from Appendix that an emission element at vector position \mathbf{r} is equivalent to a virtual one whose longitude phase shifts to an earlier value $\delta\phi(r) = \Omega\mathbf{r} \cdot \mathbf{n}_0/c$. We now calculate $\delta\phi(r)$ as a function of r , based on the dipole geometry of magnetic field configuration.

For a dipole field line, we have

$$r = \lambda \frac{cP}{2\pi} \sin^2 \Theta, \quad (1)$$

where $r = |\mathbf{r}|$, Θ is the polar angle, P the rotation period, c the speed of light, and λ a parameter which characterizes the sorts of field lines ($\lambda \gtrsim 1$, $\lambda = 1$ for the last open field lines). Based on Eq.(1), the angle Θ_μ between the direction of magnetic field at vector position \mathbf{r} and the magnetic axis μ reads,

$$\begin{aligned} \cos \Theta_\mu &= \frac{2\lambda cP - 6\pi r}{\sqrt{\lambda cP(4\lambda cP - 6\pi r)}}, \\ &= \frac{2 - 3 \sin^2 \Theta}{\sqrt{4 - 3 \sin^2 \Theta}}. \end{aligned} \quad (2)$$

Therefore, assuming that elementary emission is along magnetic field lines and according to Eq.(1-2) and Appendix, we obtain the phase shift $\delta\phi$ as a function of r

$$\delta\phi(r) = \frac{4\pi r}{\lambda cP} \sqrt{\frac{\lambda cP - 2\pi r}{4\lambda cP - 6\pi r}}, \quad (3)$$

and the phase difference $\Delta\phi$ between two emission beam components with heights r_a and r_b is

$$\Delta\phi = \delta\phi(r_a) - \delta\phi(r_b). \quad (4)$$

We note, from Eq.(3), that $\delta\phi$ is only a function of rotation period P and distance r , but is not relevant to magnetic inclination angle α and/or impact angle β . The calculations of phase shift $\delta\phi$ for pulsars with periods $P = 0.03\text{s}$, 0.05s , 0.1s , 0.5s , and 1s are shown in Fig.1.

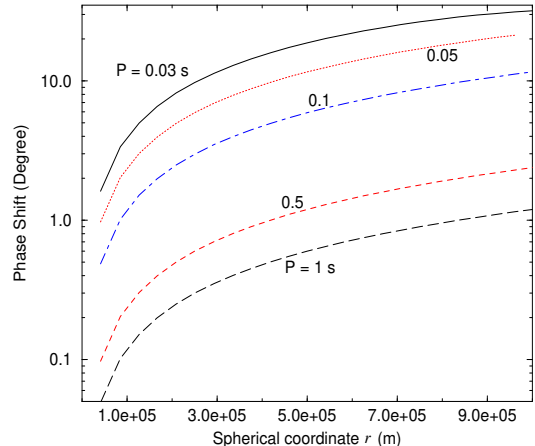


FIG. 1.— The phase shifts $\delta\phi$ for pulsars with $P = 0.03\text{s}$, 0.05s , 0.1s , 0.5s , 1s , based on Eq.(3). The emission height (spherical coordinate r) is from 30km to 10^3km . $\lambda = 1$.

We see from Fig.1 that the retardation effect arising from different emission heights is less important for pulsars with longer periods P , but can not be negligible when P is small. For instance, the phase difference between components with heights of 30km and 300km could be over 10° if $P = 30\text{ms}$. But the phase difference can only be about 1° for emission components with heights 50km and 500km if $P = 0.5\text{s}$.

2.2. The relationship between observed frequency and shifted phase

Theoretically, we can know the emission heights of beam components at a certain observation frequency

in the inverse Compton scattering model^[10,17], based on which the three components (core, inner cone, and outer cone) can be understood naturally. The frequency ν of radio wave emitted at position r (or height $r - R$, R is the pulsar radius) can be gotten by following Eq.(5-7). Low frequency electromagnetic waves with frequency ν_0 are supposed to be produced near pulsar surface due to RS-type vacuum gap sparking^[18]. These waves are assumed to propagate nearly freely in highly inhomogeneous plasma in pulsar magnetospheres and inverse Compton scattered by the secondary particles with Lorentz factor γ , turning into radio waves observed with frequency ν ^[17],

$$\nu = 1.5\gamma^2\nu_0(1 - \sqrt{1 - \gamma^{-2}} \cos \theta_i), \quad (5)$$

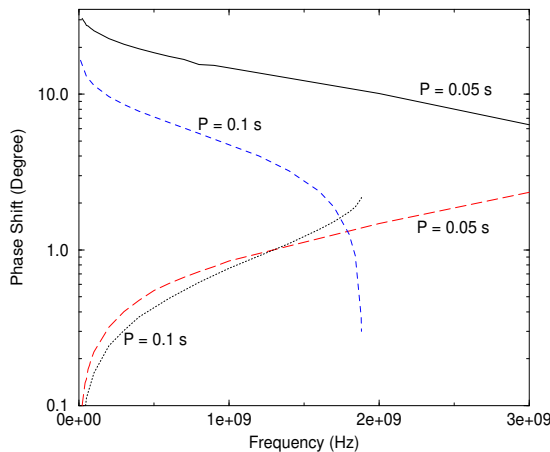
where the incident angle θ_i is the angle between the wave vector of low frequency wave and the direction of electron moving (along magnetic fields in the approximation of this paper), which can be calculated to be

$$\cos \theta_i = \frac{2 \cos \Theta + (R/r)(1 - 3 \cos^2 \Theta)}{\sqrt{(1 + 3 \cos^2 \Theta)[1 - 2(R/r) \cos \Theta + (R/r)^2]}}. \quad (6)$$

The Lorentz factor of relativistic electron should decrease with height³, which is suggested in the following form^[10]

$$\gamma = \gamma_0 \exp[-\xi \frac{r - R}{R}], \quad (7)$$

where γ_0 is the initial Lorentz factor near pulsar surface, ξ a parameter reflecting the extend of the energy loss.



³Electrons will lost their kinetic energy, via, e.g., the curvature radiation and/or the inverse Compton scattering of these electrons off thermal X-ray photons from pulsar surface, when they are moving along magnetic field lines.

⁴The position angle may jump approximately 90° if a line of sight goes nearby a singular point.

FIG. 2.— The phase differences between beam components, as functions of observation frequency, in the ICS model. The upper two lines (solid and short dashed) are the phase differences of outer cone and inner cone, while others are of inner cone and core. The pulsar periods are chosen to be 0.1s and 0.05s, and other parameters to be $\gamma_0 = 3 \times 10^3$, $\xi = 3 \times 10^{-2}$, $R = 10^4$ m, and $\nu_0 = 10^5$ Hz. $\lambda = 1$.

The relation between observation frequency ν and position r can be found from Eq.(1, 5-7). For a certain ν we may find three solutions for r : r_1, r_2, r_3 , being the positions of core, inner cone, and outer cone, respectively. The phase differences of beam components of outer and inner cones, and of inner cone and core, are calculated for observation frequency up-to a few GHz in the ICS model, which are shown in Fig.2.

We see from Fig.2 that, on one hand, at lower frequency ν , the phase differences $\Delta\phi_2 \equiv \delta\phi(r_3) - \delta\phi(r_2)$ of outer and inner cones are notable. For example, $\Delta\phi_2 = 30^\circ$ when $\nu = 2 \times 10^7$ Hz. $\Delta\phi_2$ decreases monotonously with the increase of observation frequency ν . On the other hand, the phase differences $\Delta\phi_1 \equiv \delta\phi(r_2) - \delta\phi(r_1)$ of core and inner cone components are small at lower ν . $\Delta\phi_1 = 0.05^\circ$ contrary to $\Delta\phi_2$, $\Delta\phi_1$ increases monotonously with the increase of ν . The observational tests and/or consequences of these features need further investigations in the future.

2.3. The possible distribution of singular points on the celestial sphere

There may be some points on the observational celestial sphere where the linear polarization intensity $L = 0$. We call such points as “singular points”. The polarization position angle should jump⁴ exactly 90° when a line of sight goes across one of the singular points^[7, 8]. Therefore the distribution of singular points on the celestial sphere would determine the variation properties of position angle.

Generally, it is hard to calculate the singular point distribution since there are many factors, being not well understood, to cause depolarization^[8, 19] of pulsar beamed radiation. However, if depolarization is mainly due to the incoherent superposition of emission components at different heights, and if there are only two components, we can get the singular point distribution easily in this special case.

In this case the sufficient and necessary conditions that should be satisfied at a singular point are

$$\begin{cases} \psi_1 - \psi_2 = \pm\pi/2 \\ L_1 = L_2 \end{cases}, \quad (8)$$

where ψ_i and L_i ($i = 1, 2$ denotes the first and second components, respectively) are the position angles and

linear polarization intensities of i^{th} components, respectively. The first condition, i.e., $\psi_1 - \psi_2 = \pm\pi/2$, is thus only a *necessary* one for a singular point. Considering the identity $\tan(\psi_1 - \psi_2) = \frac{\tan\psi_1 - \tan\psi_2}{1 + \tan\psi_1 \tan\psi_2}$, we can re-write the necessary condition below

$$\tan\psi_1 \tan\psi_2 = -1. \quad (9)$$

The possible distribution of singular points on the celestial sphere is calculated for this special case based on Eq.(9), and is shown in Fig.3. We assume the phase difference between the centers of the components due to their different emission heights to be $\Delta\phi = 15^{\circ}$, and the inclination angle $\alpha = 60^{\circ}$ or 30° in our calculation. We find from Fig.3 that the distribution become “flatter” when the inclination angle α is smaller, i.e., larger α may be more favorable for a line of sight to go across a singular point, thus increasing the possibility of position angle curve to “jump”.

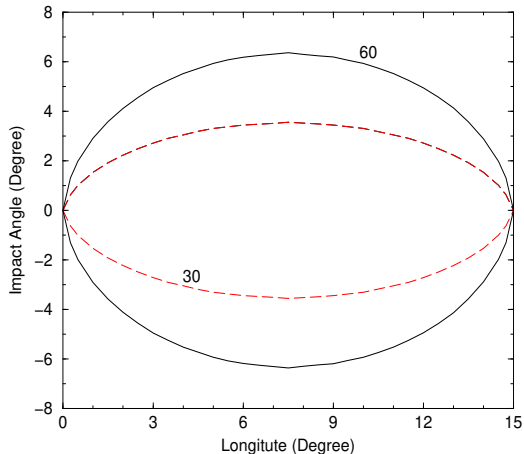


FIG. 3.— A possible distribution of singular points on the celestial sphere assuming that there are only two emission components, and that the linear depolarization arises only from the incoherent superposition of those two components. The phase difference between the components is assumed to be 15° , and the inclination angles are chosen to be 30° and 60° , respectively, in the computation.

3. EMISSION BEAMS IN THE ICS MODEL

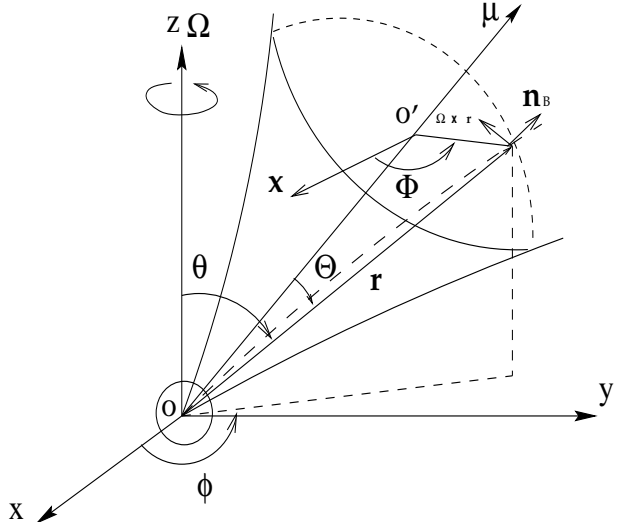


FIG. 4.— A sketch of two coordinate systems. we assume the μ -coordinate, in which the magnetic axis μ is chosen as the z -axis, turns clockwise an angle α (the inclination angle) along the x -axis of Ω -coordinate. A position vector \mathbf{r} can be represented by $\{r, \theta, \phi\}$ in Ω -coordinate, or by $\{r, \Theta, \Phi\}$ in μ -coordinate. \mathbf{n}_B is the vector unit of magnetic field.

In the above discussion, only the electron velocity along magnetic field line (the poloidal velocity) is considered. However, as a pulsar rotates, an electron does have a *toroidal* velocity (see Fig.4). Actually, the velocity of an electron in the observer rest frame can be obtained by the relativistic velocity transformation of the poloidal velocity in the rotation frame. The inclusion of such toroidal velocity has at least one implication: an emission unit would shift forward a phase with respect to the magnetic direction \mathbf{n}_B since a relativistic electron emit photon at the direction of its moving. In this section, we calculate the beam shapes modified by inclusion the toroidal velocity, based on the derived emission heights in the ICS model^[10]. In the following computation, two phase shift effects arising from different emission heights and from toroidal velocity are included. According to Fig.4, one can find the relationship between $\{\theta, \phi\}$ and $\{\Theta, \Phi\}$,

$$\begin{cases} \cos\theta &= \cos\alpha \cos\Theta - \sin\alpha \sin\Theta \sin\Phi \\ \sin\phi &= \frac{\cos\alpha \sin\Phi \sin\Theta + \sin\alpha \cos\Theta}{\sin\theta} \\ \cos\phi &= \frac{\cos\Phi \sin\Theta}{\sin\theta} \end{cases}, \quad (10)$$

which is useful below.

The linear rotation velocity at a position vector \mathbf{r} is v ,

$$\begin{aligned} v &= |\Omega \times \mathbf{r}| \\ &= \Omega r \sqrt{1 - (\cos\alpha \cos\Theta - \sin\alpha \sin\Theta \sin\Phi)^2} \end{aligned} \quad (11)$$

Thus, by the relativistic velocity transformation, one finds two components, u_1 (in the $\Omega \times \mathbf{r}$ direction) and u_2 (in the $[(\Omega \times \mathbf{r}) \times \mathbf{n}_B] \times (\Omega \times \mathbf{r})$ direction), of the

velocity of an electron in the observer rest frame,

$$\begin{aligned} u_1 &= \frac{-c\sqrt{1-\gamma^{-2}}\sin\alpha\sin\Theta\cos\Phi+v\sqrt{1+3\cos^2\Theta}}{\sqrt{1+3\cos^2\Theta}-v\sqrt{1-\gamma^{-2}}\sin\alpha\sin\Theta\cos\Phi/c}, \\ u_2 &= \frac{c\sqrt{(1-\gamma^{-2})(1-v^2/c^2)(1+3\cos^2\Theta-\sin^2\alpha\sin^2\Theta\cos^2\Phi)}}{\sqrt{1+3\cos^2\Theta}-v\sqrt{1-\gamma^{-2}}\sin\alpha\sin\Theta\cos\Phi/c}, \end{aligned} \quad (12)$$

where γ is the Lorentz factor of electron in the rotation frame. Therefore the angle δ between \mathbf{n}_B and the emitted photon is,

$$\delta\varphi = \cos^{-1}\left[\frac{-\sin\alpha\sin\Theta\cos\Theta}{\sqrt{1+3\cos^2\Theta}}\right] - \cos^{-1}\left[\frac{u_1}{\sqrt{u_1^2+u_2^2}}\right], \quad (13)$$

which is also the phase shift due to toroidal velocity.

Combining the phase shifts of $\delta\phi$ (Eq.(3)) and $\delta\varphi$ (Eq.(13)), we can calculate the emission beams in the ICS model. We use the results in Fig.2 to decide the emission heights. The radio emission is assumed to originated from a region between magnetic field lines denoted by $\lambda = 1$ and that by $\lambda = 1.8$. The radius of the stellar surface of the feet of the field lines corresponding to $\lambda = 1.8$ is $\sim \lambda^{-1/2}\theta_p \sim 0.75\theta_p$, where $\theta_p = \sin^{-1}\sqrt{\frac{2\pi R}{cP}}$ is the radius of polar cap. The cases of rotation period $P = 0.1s$ and $0.05s$, and observation frequency $\nu = 10^9\text{Hz}$ are presented in Fig.5 and Fig.6. The parameters in the simulation are listed in Table 1.

From Fig.5 and Fig.5, we see the emission beams are clearly *not* symmetric although the emission regions of these components may be symmetric respect to the magnetic axes. The width of the first pulse in a conal component would be much smaller than that of the second one. Besides the clear phase shifts between the components, the emission beams may not have circular cross sections when the rotation period is small (see Fig.6). The pulses of impact angle $\beta > 0$ arrive earlier than that of $\beta < 0$. This is understandable. Since the emission region of $\beta > 0$ is farther from the rotation axis than that of $\beta < 0$, the phase shift effect thus is more remarkable due to larger toroidal velocity.

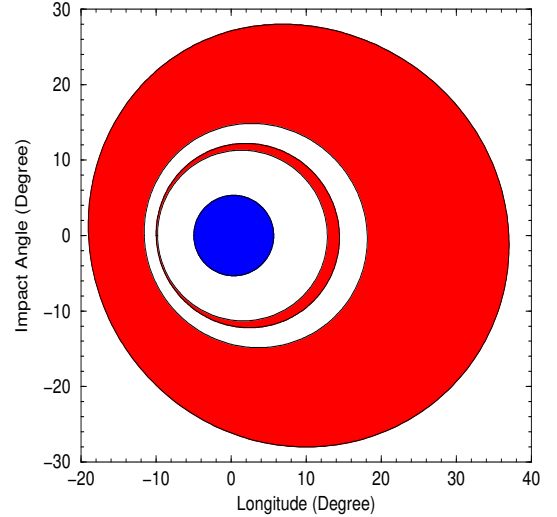


FIG. 5.— The emission beams of core, inner cone, and outer cone simulated in the ICS model, with the inclusion of the phase shift effects both due to different emission heights and to toroidal velocity. The inclination angle $\alpha = 30^\circ$, the rotation period $P = 0.1\text{s}$. Other parameters are the same as in Fig.2.

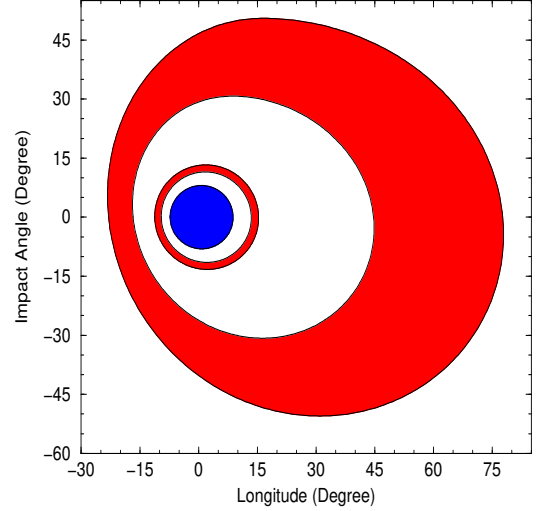


FIG. 6.— Same as in Fig.5, but for $P = 0.05\text{s}$.

4. CONCLUSION AND DISCUSSION

A detail consideration of the relative longitude phase shift due to different emission heights of three components is presented in this paper. Our main conclusion can be summarized below.

1, An emission unit along direction $\mathbf{n}_1(\theta_0, \phi_1)$ at an arbitrary position \mathbf{r}_1 arrives earlier than another emission unit along direction $\mathbf{n}_2(\theta_0, \phi_2)$ at another position \mathbf{r}_2 , the phase difference between those two elements is $\phi_1 - \phi_2 + \Omega(\mathbf{n}_1 \cdot \mathbf{r}_1 - \mathbf{n}_2 \cdot \mathbf{r}_2)/c$ (*if* this value is positive), where Ω is the rotational angular velocity.

TABLE 1

THE PARAMETERS* CHOSEN AND CALCULATED IN THE ICS MODEL FOR THE COMPUTATIONS OF EMISSION BEAM COMPONENTS

* P - rotation period; ν - observation frequency; r_i - emission height of component i ; $i = 1, 2, 3$ denotes core, inner cone, and outer cone, respectively; $\theta_{\mu i}$ - angular radius of component i ; $\Delta\phi_1$ and $\Delta\phi_2$ are the phase differences of core and inner cone, and of inner and outer cones, respectively.

P (s)	ν (Hz)	r_1 (m)	r_2 (m)	r_3 (m)	$\theta_{\mu 1}$	$\theta_{\mu 2}$	$\theta_{\mu 3}$	$\Delta\phi_1$	$\Delta\phi_2$
0.1	10^9	18820	81900	483820	$5^\circ.4$	$11^\circ.3$	$28^\circ.1$	$0^\circ.76$	$4^\circ.74$
0.05	10^9	20695	56040	697000	$8^\circ.0$	$13^\circ.2$	$50^\circ.5$	$0^\circ.85$	$14^\circ.71$

2, The phase shift effect is less important when the rotation period $P > 0.5$ s.

3, The phase shift values, as a function of observation frequency ν , are presented in the ICS model. As ν increases, the shift between outer and inner cones decreases, while the shift between inner cone and core increases.

4, Larger inclination angles may be favorable for the appearance of polarization position angle jumps.

6, The emission beams are not symmetric in the ICS model, which is achieved by the inclusion of the phase shift effects both due to different emission heights and to toroidal velocity ($\Omega \times \mathbf{r}$).

In the simulation of the beam shapes of this paper, we just take the symmetric emission region in the ICS model for simplicity. However, the emission region should actually *not* be symmetric respect to the magnetic axes when we consider that, for a certain inverse Compton scattering process, the low-frequency wave is emitted at an earlier sparking point, and that electrons are not moving exactly along magnetic field lines. How about the emission beams and polarization properties when these issues are included? A further study is needed in the future.

acknowledgements: We thank our pulsar group for discussions.

Appendix

Observation shows that emission components (core, inner cone, and outer cone) could come from different heights^[9]. The longitude phase shifts between those components are thus inevitable^[7]. We now try to determine this shift value between two emission components. Our measures to deal with this question is

⁵We call two emission units are equivalent only if an observer at infinity can not distinguish them, i.e., the observer detects same intensity at same time for those two emission units.

that: first we find a virtual equivalent⁵ at origin for an emission unit at arbitrary position; then we compare the phases of the virtual equivalents. The phase difference between two virtual equivalents is actually the phase difference observed of those two corresponding emission units. Our conclusion can be expressed as following proposition:

An emission unit along a direction $\mathbf{n}_0(\theta_0, \phi_0)$ at an arbitrary position $\mathbf{r}(\theta, \phi)$ is equivalent observationally to a virtual emission unit along direction $\mathbf{n}'_0(\theta_0, \phi'_0)$ at origin, where $\phi'_0 = \phi_0 + \Omega\tau$, $\tau = \mathbf{r} \cdot \mathbf{n}_0/c$, Ω and c are the rotational angular velocity and the speed of light, respectively.

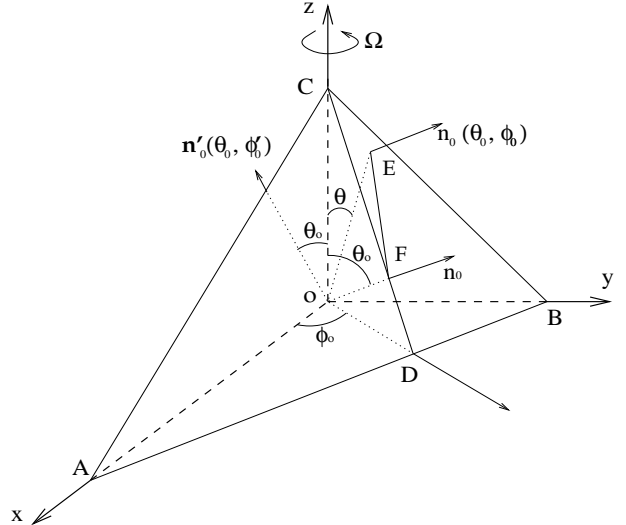


FIG. 7.— A sketch geometrical figure for proving the conclusion to find an equivalent emission unit at origin. An emission along \mathbf{n}_0 at point E (position vector \mathbf{r}) is equivalent to the virtual one along \mathbf{n}'_0 at origin.

We are to prove this below. As in Fig.7, we erect coordinates o-xyz in the observation rest frame, where z-axis is along rotational axis (Ω), the origin is at

the center of pulsar. We are considering the emission along \mathbf{n}_0 at an arbitrary point E. A plane ABC is created so that \mathbf{n}_0 is perpendicular to this plane. Because all emission units along the direction \mathbf{n}_0 at those points which are on the ABC plane should be observed simultaneously, the emission along \mathbf{n}_0 at point⁶ F is equivalent to the emission at point E if the intensities are the same. We assume the time $t = 0$ when a photon is emitted at point E along \mathbf{n}_0 . A photon emitted at point O along \mathbf{n}_0 when $t = -\tau$ ($\tau = |\mathbf{OF}|/c$) arrives at point F when $t = 0$ (still along \mathbf{n}_0). However, at $t = 0$, the emission at point O is along $\mathbf{n}'_0(\theta_0, \phi_0 + \Omega\tau)$ because of rotation. Therefore, an emission along \mathbf{n}_0 at point E with position vector \mathbf{r} is equivalent to the virtual one along \mathbf{n}'_0 at origin O.

Now we calculate the value τ . In the right-angled triangle OEF, $|\mathbf{OF}| = \mathbf{r} \cdot \mathbf{n}_0$. We thus have $\tau = \mathbf{r} \cdot \mathbf{n}_0 / c$.

REFERENCES:

1. Radhakrishnan V., Cooke, D.J., *Astrophys. Lett.*, 1969, 3, 225
2. Ferguson, D.C. *Astrophys. J.*, 1976, 205, 247
3. Blaskiewicz, M., Cordes, J.M., Wasserman, I. *Astrophys. J.*, 1991, 307, 643
4. Hibschman, J.A., Arons, J. *Astrophys. J.*, 2001, in press (astro-ph/0008117)
5. Stinebring D.R., et al. *Astrophys. J. Suppl.*, 1984, 55, 247
6. Mckinnon, M.M., Stinebring D.R. *Astrophys. J.*, 1998, 502, 883
7. Xu, R.X., Qiao, G.J., Han, J.L. *Astron. & Astrophys.*, 1997, 323, 395
8. Xu, R.X., Qiao, G.J. *Science in China*, 2000, A43, 439
9. Rankin, J.M. *Astrophys. J.*, 1983, 274, 333
10. Qiao, G.J., Lin, W.P. *Astron. & Astrophys.*, 1998, 333, 172
11. Jones, P.B., *Astrophys. J.*, 1980, 236, 661
12. Narayan R., Vivekanand M., *A&Ap*, 1983, 122, 45
13. Lyne A.G. & Manchester R.N., *Mon.Not.Roy.Astr.Soc.*, 1988, 234, 477
14. Biggs, J.D., *Mon.Not.Roy.Astr.Soc.*, 1990, 245, 514
15. Wu X.J., Shen J.X., *Kexue Tongbao*, 1988, 20, 1567 (in Chinese)
16. Rankin J.M., *Astrophys. J.*, 1993, 405, 285
17. Xu, R.X., Liu, J.F., Han, J.L., Qiao, G.J. *Astrophys. J.*, 2000, 535, 354
18. Ruderman, M.A., Sutherland, P.G. *Astrophys. J.*, 1975, 196, 51
19. Lyutikov, M. *Astrophys. J.*, 1999, 525, L37

⁶Point F is the intersection of ABC plane and its perpendicular line through point O.